

Influence of the Polyamino Carboxylate Chelating Ligand (L) on the Kinetics and Mechanism of the Formation of Fe^{II}(L)NO in the System Fe^{II}(L)/NO/HONO/NO₂⁻ in Aqueous Solution

V. Zang and R. van Eldik*

Received November 21, 1989

Fe^{II}(L) reacts with NO, HONO, and NO₂⁻ to produce Fe^{II}(L)NO for L = diethylenetriaminepentaacetate, ethylenediaminetetraacetate, *N*-(hydroxyethyl)ethylenediaminetriacetate, nitrilotriacetate, ethylenediaminediacetate, and water. The reaction with HONO and NO₂⁻ occurs in two parallel paths of different order with respect to the reaction components. The systematic variation of the nature of L enables an investigation of the role of labile coordination sites on the Fe(II) center during such reactions. The parallel reactions are characterized by the rate law $-d[\text{Fe}^{\text{II}}(\text{L})]/dt = k_A[\text{HONO}]^2 + k_B[\text{Fe}^{\text{II}}(\text{L})][\text{HONO}]$, and the contribution of each path depends on the nature of L, pH, and total nitrite concentration. The kinetic data support the formation of a reactive intermediate, most probably N₂O₃ (*k*_A path), and the reduction of HONO by Fe^{II}(L) to NO (*k*_B path). The observed reactions and reactivity patterns strongly depend on the availability of labile coordinated solvent molecules on Fe^{II}(L), as governed by the nature of the ligand L. The results of this study are discussed in reference to the available literature data and in comparison to the kinetics of oxidation of these complexes by molecular oxygen.

Introduction

In general, we are interested in the catalytic role of metal ions and complexes in homogeneous redox reactions involving SO_x and NO_x species. These processes are of atmospheric relevance in terms of either acid rain formation¹ or the simultaneous removal of these species from gaseous effluents of coal-fired power plants.²⁻⁴ Metal ions and complexes can not only catalyze such processes but also increase the degree of absorption of NO via direct coordination to the metal center, since NO is rather insoluble in water.^{5,6} The mechanisms of such reactions are in general complicated and not at all well understood. This partly restricts further development and systematic modification of the catalytic properties of the metal complexes.

Following our earlier studies on the complex formation and subsequent redox kinetics of the Fe(III)-SO_x system,⁷⁻⁹ we recently reported a detailed study of the formation of Fe^{II}(edta)NO (edta = ethylenediaminetetraacetate) in the system Fe^{II}(edta)/NO/HONO/NO₂⁻ in aqueous solution.¹⁰ This reaction occurs in two parallel paths of different order, viz. pseudo first and pseudo zero order in the Fe^{II}(edta) concentration, respectively. The kinetics of the reaction can be described by the rate law $-d[\text{Fe}^{\text{II}}(\text{edta})]/dt = k_A[\text{HONO}]^2 + k_B[\text{Fe}^{\text{II}}(\text{edta})][\text{HONO}]$, where *k*_A and *k*_B have the values 62 and 90 M⁻¹ s⁻¹, respectively, at 25 °C and 0.5 M ionic strength. The suggested mechanism for the parallel reaction paths involves rate-determining formation of NO⁺ or N₂O₃ and the reduction of HONO to NO by Fe^{II}(edta), respectively. In this respect, it is interesting to note that there has been much interest lately in the reduction of nitrite by various transition-metal complexes,¹¹⁻¹⁹ involving reactions similar to those reported in our earlier and present studies.

We have now systematically varied the nature of the polyamino carboxylate ligand (L) to study its influence on the kinetics and mechanism of the formation of Fe^{II}(L)NO in the system Fe^{II}(L)/NO/HONO/NO₂⁻ in aqueous solution. The selected ligands include dtpa (diethylenetriaminepentaacetate), hedtra (*N*-(hydroxyethyl)ethylenediaminetriacetate), nta (nitrilotriacetate), and edda (ethylenediaminediacetate). By way of comparison, the corresponding reactions were also studied for the aquated Fe(II) ion, i.e. in the absence of a polyamino carboxylate ligand. The results of this study allow us to make an overall comparison and to draw important conclusions regarding the ligand sensitivity of such processes.

Experimental Section

Materials. Chemicals of analytical reagent grade and deionized water were used throughout this study. The Fe^{II}(L) complexes were prepared in solution from FeSO₄ and H₂dtpa, Na₂H₂edta, Na₃hedtra, H₃nta, and H₂edda. For the aquated Fe(II) species, Fe(ClO₄)₂ was used. Acetic acid/sodium acetate buffers were used to control the pH of the test solution, whereas HClO₄ was used in more acidic solutions. NaClO₄ was used to adjust the ionic strength of the medium.

Preparation of Solutions. All the Fe^{II}(L) complexes studied are extremely oxygen-sensitive and are rapidly oxidized to Fe^{III}(L). In order to minimize this complication, solutions were prepared as described previously.¹⁰ The Fe^{II}(L)NO complexes were also prepared and handled as described for the Fe^{II}(edta)NO complex.¹⁰

Spectroscopic and Kinetic Measurements. UV-vis spectra and slow kinetic measurements were performed in gastight cuvettes in the thermostated (±0.1 °C) cell compartment of a Shimadzu UV 250 spectrophotometer. Short-lived intermediates were studied with the aid of a OSMA rapid-scan spectrometer (Spectroscopic Instruments GmbH, Gilching, FRG) coupled to a Durrum D 110 stopped-flow unit. This system permits the recording of complete spectra in the range 250-550 nm at 16-ms intervals. IR studies on aqueous solutions of Fe^{II}(L)NO were performed with the aid of an ATR cell (Harrick) and a Nicolet 5 SX FT-IR instrument. Fast kinetic measurements were performed on a modified Aminco and a Durrum D 110 stopped-flow instrument, using an on-line data acquisition system.²⁰ Under specific experimental con-

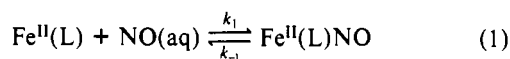
- (1) Sigg, L.; Stumm, W.; Zobrist, J.; Zürcher, F. *Chimia* **1987**, *41*, 159.
- (2) Sada, E.; Kumazawa, H.; Takada, Y. *Ind. Eng. Chem. Fundam.* **1984**, *23*, 60.
- (3) Sada, E.; Kumazawa, H.; Hikosaka, H. *Ind. Eng. Chem. Fundam.* **1986**, *25*, 386.
- (4) Sada, E.; Kumazawa, H.; Machida, H. *Ind. Eng. Chem. Res.* **1987**, *26*, 2016.
- (5) Littlejohn, D.; Chang, S. G. *J. Phys. Chem.* **1982**, *86*, 537.
- (6) Chang, S. G.; Littlejohn, D.; Lynn, S. *Environ. Sci. Technol.* **1983**, *17*, 649.
- (7) Kraft, J.; van Eldik, R. *Inorg. Chem.* **1989**, *28*, 2297, 2306.
- (8) Kraft, J.; van Eldik, R. *Atmos. Environ.* **1989**, *23*, 2709.
- (9) Dellert, M.; van Eldik, R. Submitted for publication.
- (10) Zang, V.; Kotowski, M.; van Eldik, R. *Inorg. Chem.* **1988**, *27*, 3279. There is a printing error in this paper: In Table I *k*_{obs} = 0.0015 ± 0.0001 s⁻¹ at pH = 4.70; the quoted value is for the next entry at pH = 5.30.
- (11) Stedman, G. *Adv. Inorg. Chem. Radiochem.* **1979**, *22*, 143.
- (12) Hishinuma, Y.; Kayi, R.; Akimoto, H.; Nakajima, F.; Mori, T.; Kamo, T.; Arikawa, Y.; Nozawa, S. *Bull. Chem. Soc. Jpn.* **1979**, *52*, 2863.

- (13) Ogino, H.; Tukahara, K.; Tanaka, N. *Bull. Chem. Soc. Jpn.* **1974**, *47*, 2863.
- (14) Melton, J. D.; Bakac, A.; Espenson, J. H. *Inorg. Chem.* **1986**, *25*, 3360.
- (15) Hyde, M. R.; Garner, C. D. *J. Chem. Soc., Dalton Trans.* **1975**, 1186.
- (16) Barley, M. H.; Takeuchi, K. H.; Meyer, T. J. *J. Am. Chem. Soc.* **1986**, *108*, 5876.
- (17) Epstein, I. R.; Kustin, K.; Warshaw, L. J. *J. Am. Chem. Soc.* **1980**, *102*, 3751.
- (18) Uchiyama, S.; Muto, G.; Nozaki, K. *J. Electroanal. Chem. Interfacial Electrochem.* **1978**, *91*, 301.
- (19) Hughes, M. N.; Shrimanker, K.; Wimbledon, P. E. *J. Chem. Soc., Dalton Trans.* **1978**, 1634.
- (20) Kraft, J.; Wieland, S.; Kraft, U.; van Eldik, R. *GIT Fachz. Lab.* **1987**, *31*, 560.

ditions, parallel zero- and first-order reactions were observed, and these data were treated on an Atari Mega 4 computer as outlined previously.¹⁰

Results and Discussion

Preliminary Observations. All the investigated polyamino carboxylate complexes of Fe(II) exhibit a significant reaction with oxygen, and a detailed report is given elsewhere.²¹ In general, these complexes are oxidized by oxygen to the Fe^{III}(L) species. It is therefore absolutely necessary to work under O₂-free conditions when the Fe^{II}(L)/NO/HONO/NO₂⁻ system is investigated, since the corresponding Fe^{III}(L) species do not react with NO. All complexes including the aquated Fe(II) ion react extremely rapidly with NO to produce Fe^{II}(L)NO.^{5,6,12,22} In the case of Fe(H₂O)₆²⁺, $k_1 = 7 \times 10^5 \text{ M}^{-1} \text{ s}^{-1}$ and $k_{-1} = 1.5 \times 10^3 \text{ s}^{-1}$ such that $K_1 = k_1/k_{-1} = 4.7 \times 10^2 \text{ M}^{-1}$.⁶ By way of comparison, the value of K_1 for Fe^{II}(edta)NO is significantly larger (the rate constants are too high for *T*-jump measurements), viz. $1 \times 10^6 \text{ M}^{-1}$.^{5,12} In general, K_1 values decrease with decreasing number of potential binding sites on the chelate ligand, with the exception of those of Fe(dtpa)NO. We studied the kinetics of reaction 1 for L = dtpa using stopped-flow and *T*-jump techniques



and found $k_1 = (2.7 \pm 0.2) \times 10^5 \text{ M}^{-1} \text{ s}^{-1}$ and $k_{-1} = 23 \pm 11 \text{ s}^{-1}$ at 25 °C. The latter value cannot be determined accurately and should be treated as an upper limit, such that the K_1 value of $1.2 \times 10^4 \text{ M}^{-1}$ at pH = 5 is a lower limit. In addition, the values of K_1 parallel the stability constants of the Fe^{II}(L) complexes.^{23,24} These trends demonstrate the important influence of the chelation effect on the magnitude of k_1 , since k_{-1} is less sensitive toward the nature of L.

The reactions of Fe^{II}(L) with HONO/NO₂⁻ are significantly slower than those with NO and can be studied conveniently by using stopped-flow techniques. Here again, the reaction product Fe^{II}(L)NO is the same as produced during the reaction with NO. IR and UV-vis spectroscopic investigations underline this statement. The IR spectra of aqueous solutions of Fe^{II}(L)NO exhibit characteristic NO vibrations at 1775 (L = dtpa, edta, hedtra), 1793 (L = nta), and 1808 cm⁻¹ (L = H₂O). Thus the force constant for the NO vibration increases along the series, indicating a decrease in Fe-NO bond strength. A comparison with literature values²⁵ indicates that a linear Fe-N-O structure is plausible. Simultaneously, the carboxylate vibrations in Fe^{II}(L) are influenced characteristically by the binding of NO. The antisymmetric vibration of the carboxylate groups around 1590 cm⁻¹ is shifted to higher wavenumbers, whereas the symmetric vibration at 1400 cm⁻¹ is shifted to lower wavenumbers during the formation of Fe^{II}(L)NO. This indicates an increased stabilization of the Fe^{II}(L) complex on the binding of NO,²⁶ which is in agreement with the decreased oxidation sensitivity observed for these complexes. The UV-vis spectra of Fe^{II}(L)NO exhibit charge-transfer absorption bands around 435 nm ($\epsilon = 670\text{--}750 \text{ M}^{-1} \text{ cm}^{-1}$) that systematically shift along the series of complexes to higher wavelengths (L = nta (438 nm), edda (440 nm), H₂O (450 nm)). According to these data, the stability of the Fe^{II}(L)NO complex, as well as the nitrosyl character of coordinated NO, seems to increase with increasing stability of the Fe^{II}(L) species. This trend suggests the possible formation of Fe^I(L)(NO⁺) species for the more stable complexes.^{23,27}

The formation of Fe^{II}(L)NO via the reaction of Fe^{II}(L) with HONO/NO₂⁻ is accompanied by the formation of Fe^{III}(L) in the approximate ratio of 1:1. No Fe^{III}(L) is produced during the reaction of Fe^{II}(L) with NO(aq). In the case of a mixture of

NO/HONO/NO₂⁻, Fe^{II}(L) rapidly reacts with the available NO, followed by a slower step, during which 50% of the remaining Fe^{II}(L) is converted to Fe^{II}(L)NO and the rest to Fe^{III}(L). The Fe^{II}(L)NO complexes are very stable in the presence of an excess of Fe^{II}(L) but decompose to Fe^{III}(L) in the presence of an excess of HONO/NO₂⁻. Under no circumstances was Fe^{III}(L) found to be produced during the reaction of Fe^{II}(L) with NO. In acidic medium, nitrite disproportionates into NO and NO₃⁻, which accounts for the partial formation of NO under such conditions. In order to prevent this complication, the Fe^{II}(L) stock solutions rather than the nitrite solutions were acidified prior to mixing.

An aspect of fundamental importance to this study concerns the coordination geometry of the Fe^{II}(L) species. In our earlier study of the edta system,¹⁰ we presented arguments in favor of the presence of a water molecule in the coordination sphere of the Fe^{II}(edta) species, i.e. Fe^{II}(edta)H₂O. A pH titration of this complex indicated the partial formation of a ring-opened, protonated complex Fe^{II}(Hedta) at pH < 3. Furthermore, there was no evidence for a coordinated water molecule with a p*K*_a value lower than 9.5. It is uncertain whether the edta ligand in this complex occupies five or six coordination sites, the latter being the case for Fe^{III}(edta)H₂O.^{28,29} An increase in the number of potential binding sites on the chelate ligand, as in the case of dtpa, will diminish the possibility of a coordinated water molecule. In the case of the Fe^{II}(dtpa) complex, the crystal structure indicates a complex without a coordinated water molecule, but with heptacoordination involving four carboxylate groups and three N atoms.³⁰ Further information on the structure of Fe^{II}(dtpa) in solution was obtained from a pH titration of a 0.002 M Fe^{II}/H₂dtpa³⁻ mixture. The initial pH of 3.3 indicates that approximately 25% of the complex exists as Fe^{II}(Hdtpa⁴⁻) and the remainder as Fe^{II}(H₂dtpa³⁻). The titration with base exhibits two clear equivalent points with p*K*_a values of 3.5 and 5.7 ascribed to the deprotonation of the first and second protons on the coordinated H₂dtpa³⁻ ligand, respectively. The latter value is in good agreement with a value of 5.4 reported in the literature.³¹ It follows that protonation of the dtpa ligand at pH < 4 could lead to the formation of a hexacoordinated species (three carboxylate and three N coordination sites) with or without the presence of a water molecule. No evidence for the presence of such a water molecule with a p*K*_a value lower than 10 was found. These results are in agreement with the kinetic study described above. The reaction of NO with Fe^{II}(dtpa) is significantly slower than that with Fe^{II}(edta), and the oxidation reaction with O₂ exhibits the same trend.²¹ The most likely explanation is that one coordination site of Fe^{II}(edta) is occupied by a labile water molecule, whereas this is not the case for the Fe^{II}(dtpa) complex.

A decrease in the number of binding sites on L, as for hedtra, nta, and edda, will enable the coordination of one or more water molecules. In a parallel study of the substitution behavior of complexes of the type Ru^{III}(L), L = edta, hedtra, and medtra (*N*-methylthylenediaminetriacetate), the systematic variation of L significantly influenced the lability of the coordinated water molecule and controlled the kinetics of the substitution process.³²⁻³⁴ It is safe to conclude that the Fe(II) complex of hedtra will at least have one coordinated water molecule, whereas the nta and edda complexes will have two such molecules in their coordination spheres. pH titrations of these complexes under rigorous exclusion of oxygen provided no evidence for a coordinated water molecule with a p*K*_a value lower than 9.5. This is in agreement with that reported in the literature³⁵ and generally observed for Fe(II)-aqua

- (21) Zang, V.; van Eldik, R. *Inorg. Chem.* **1990**, *29*, 1705.
 (22) Lin, N. H.; Littlejohn, D.; Chang, S. G. *Ind. Eng. Chem. Process Des. Dev.* **1982**, *21*, 725.
 (23) Ogura, K.; Watanabe, M. *Electrochim. Acta* **1982**, *27*, 111.
 (24) Ogura, K.; Ozeki, T. *Electrochim. Acta* **1981**, *26*, 877.
 (25) Weidlein, J.; Müller, U.; Dehnicke, K. *Schwingungsfrequenzen 1*; Thieme: Stuttgart, FRG, 1981.
 (26) Sawyer, D. T.; McKinnie, J. M. *J. Am. Chem. Soc.* **1960**, *82*, 4191.
 (27) McCleverty, J. A. *Chem. Rev.* **1979**, *79*, 53.

- (28) Hoard, J. L.; Lind, M.; Silverton, J. V. *J. Am. Chem. Soc.* **1961**, *83*, 2770.
 (29) Lind, M. D.; Hoard, J. L.; Hamor, M. J.; Hamor, T. A. *Inorg. Chem.* **1964**, *3*, 34.
 (30) Schuklanova, E. B.; Polynova, T. N.; Poznyak, A. L.; Dikareva, L. M.; Porai-Koshits, M. A. *Koord. Khim.* **1981**, *7*, 1729.
 (31) Kurimura, Y.; Ochiai, R.; Matsuura, N. *Bull. Chem. Soc. Jpn.* **1968**, *41*, 2334.
 (32) Bajaj, H. C.; van Eldik, R. *Inorg. Chem.* **1988**, *27*, 4052.
 (33) Bajaj, H. C.; van Eldik, R. *Inorg. Chem.* **1989**, *28*, 1980.
 (34) Bajaj, H. C.; Eldik, R. *Inorg. Chem.* **1990**, *29*, 2855.
 (35) Schwarzenbach, G.; Heller, J. *Helv. Chim. Acta* **1951**, *34*, 1889.

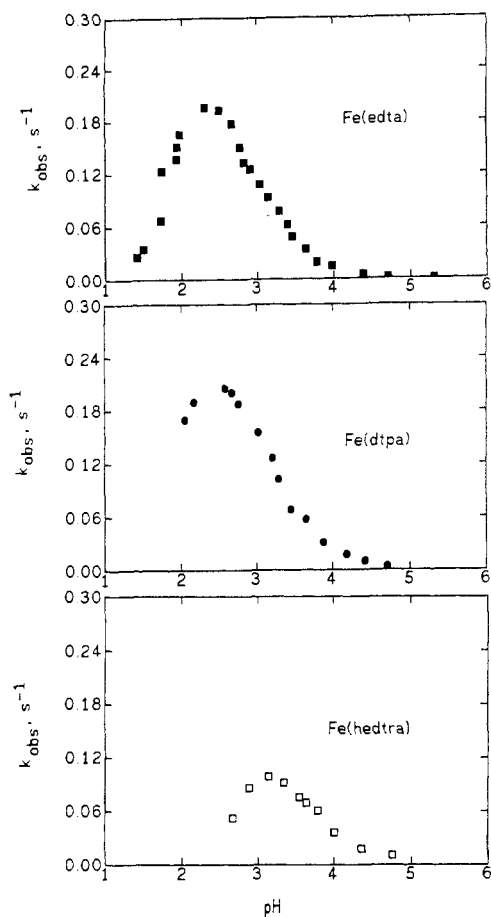


Figure 1. pH dependence of k_{obs} for the formation of $\text{Fe}^{\text{II}}(\text{L})\text{NO}$. Conditions: $[\text{Fe}(\text{L})] = 5 \times 10^{-3} \text{ M}$; $[\text{total NO}_2^-] = 5 \times 10^{-4} \text{ M}$; temperature 25°C ; ionic strength 0.5 M .

species. It follows that the deprotonation of coordinated water molecules in the investigated complexes is not expected to occur at $\text{pH} < 9.5$.

Kinetic Measurements. A detailed kinetic study of the system $\text{Fe}^{\text{II}}(\text{L})/\text{NO}_2^-/\text{HONO}$ was undertaken under the conditions selected previously,¹⁰ viz. 25°C and 0.5 M ionic strength. All reactions were studied under pseudo-first-order conditions, i.e. with either $\text{Fe}^{\text{II}}(\text{L})$ or $\text{HONO}/\text{NO}_2^-$ in at least 10-fold excess. Under these conditions, systematic concentration and pH dependence studies were undertaken.

When $\text{Fe}^{\text{II}}(\text{L})$ is in excess for $\text{L} = \text{dtpa}$ and hedtra , and absorbance/time plots at 435 nm are typical for a pseudo-first-order reaction and the corresponding $\ln(A_\infty - A_t)$ versus t plots linear for at least 2–3 half-lives of the reaction. The available data are presented as a function of pH in Figure 1 along with the data for the corresponding edta system.¹⁰ The latter series of data has now been extended to lower pH by using NaClO_4 instead of Na_2SO_4 to adjust the ionic strength and HClO_4 to adjust the acidity of the medium. Acetate buffers were used at $\text{pH} > 3.4$, and control experiments in the absence of buffer indicated no significant buffer effects on the value of k_{obs} , except for the fact that there is a significant pH drift under such conditions in the absence of buffer. The almost complete bell-shaped pH dependence now reported for the reaction of $\text{Fe}^{\text{II}}(\text{edta})$ clearly demonstrates the operation of various acid–base equilibria that affect the kinetics of the process as suggested previously.¹⁰ The decrease in k_{obs} with increasing $[\text{H}^+]$ at $\text{pH} < 2.3$ is ascribed to the protonation and dechelation of the edta ligand, accompanied by a significant decrease in lability. The data in Figure 1 would suggest a protonation constant of $\text{p}K \approx 2$, which is in good agreement with recent literature information.³⁶ The $\text{Fe}^{\text{II}}(\text{dtpa})$ system exhibits a very similar pH

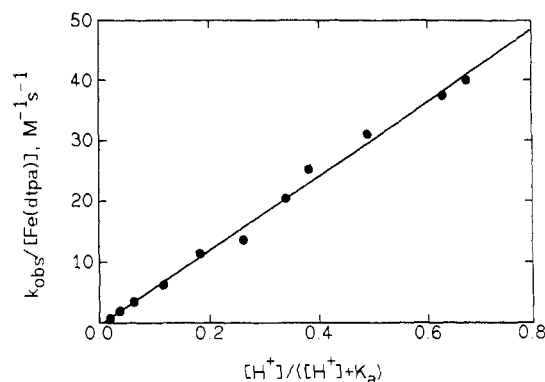
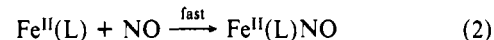
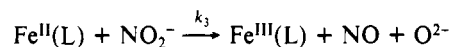
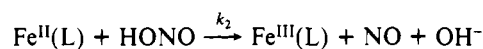
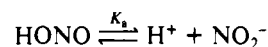


Figure 2. Plot of $k_{\text{obs}}/[\text{Fe}(\text{dtpa})]$ versus $[\text{H}^+]/([\text{H}^+] + K_a)$.

dependence with a significantly higher reactivity at $\text{pH} > 3$. In the case of the hedtra complex, the increase in k_{obs} with decreasing pH reaches a maximum at $\text{pH} \approx 3.2$, after which k_{obs} decreases drastically on increasing the $[\text{H}^+]$. This trend is ascribed to an earlier protonation and dechelation of the hedtra ligand in agreement with the significantly smaller stability constant of this complex as compared to the edta and dtpa species.^{23,24}

The general decrease in k_{obs} with increasing pH observed in Figure 1 is ascribed to the different redox capabilities of HONO and NO_2^- , as suggested previously¹⁰ and as reflected by their redox potentials of 0.99 and -0.46 V , respectively.³⁷ According to the suggested mechanism in (2) and the corresponding rate law in (3), a sigmoid-shaped pH dependence is expected around $\text{pH} =$



$$k_{\text{obs}} = \frac{k_2[\text{H}^+] + k_3K_a}{[\text{H}^+] + K_a} [\text{Fe}^{\text{II}}(\text{L})] \quad (3)$$

$\text{p}K_a = 3$.¹⁰ The data in Figure 1 qualitatively fit the expected pH dependence when the protonation/dechelation of the ligand L at lower pH is taken into consideration. According to the results in Figure 1, k_{obs} decreases to zero at high pH, indicating that $k_2 \gg k_3$. Under such conditions eq 3 simplifies to eq 4, according

$$k_{\text{obs}} = k_2[\text{H}^+][\text{Fe}^{\text{II}}(\text{L})]/([\text{H}^+] + K_a) \quad (4)$$

to which a plot of $k_{\text{obs}}/[\text{Fe}^{\text{II}}(\text{L})]$ versus $[\text{H}^+]/([\text{H}^+] + K_a)$ should be linear with slope k_2 . This is indeed the case for the data in Figure 1 over a limited pH range, i.e. where the protonation/dechelation of L does not interfere. Such a plot is presented for $\text{L} = \text{edta}$ elsewhere¹⁰ and for $\text{L} = \text{dtpa}$ in Figure 2. The values of k_2 obtained in this way for the pH range indicated in parentheses are 45 ± 3 ($\text{L} = \text{edta}$, $\text{pH} > 2.6$),¹⁰ 61 ± 2 ($\text{L} = \text{dtpa}$, $\text{pH} > 2.6$), and $83 \pm 6 \text{ M}^{-1} \text{ s}^{-1}$ ($\text{L} = \text{hedtra}$, $\text{pH} \geq 3.8$). The plots do not exhibit meaningful intercepts, which indicates that our assumption that $k_2 \gg k_3$ is correct. The experimental data were also fitted with eq 3 by plotting $k_{\text{obs}}([\text{H}^+] + K_a)/[\text{Fe}^{\text{II}}(\text{L})]$ versus $[\text{H}^+]$, and here also the intercepts k_3 were negligible.

A significant observation from the data in Figure 1 and the above calculations is the increased reactivity (k_2) for $\text{L} = \text{dtpa}$ and hedtra compared to that of $\text{L} = \text{edta}$. This is especially seen in the data at higher pH. According to the mechanism in (2), the rate-determining steps involve the reduction of (mainly) HONO and NO_2^- by $\text{Fe}^{\text{II}}(\text{L})$ to produce NO and $\text{Fe}^{\text{III}}(\text{L})$, followed by the rapid formation of $\text{Fe}^{\text{II}}(\text{L})\text{NO}$. The reaction products $\text{Fe}^{\text{II}}(\text{L})\text{NO}$ and $\text{Fe}^{\text{III}}(\text{L})$ are produced in the ratio 1:1, and the mechanism also accounts for the increase in pH observed during

(36) Marton, A.; Südkösd-Rozlosnik, N.; Vértés, A.; Nagy-Czakó, I.; Burger, K. *Inorg. Chim. Acta* **1987**, *137*, 173.

(37) *Handbook of Chemistry and Physics*, 62nd ed.; CRC: Boca Raton, FL, 1981; p d-133.

Table I. Dependence of k_{obs} on $[\text{Fe}^{\text{II}}(\text{L})]$ for Reaction 2 in the Presence of Excess $\text{Fe}^{\text{II}}(\text{L})^a$

$[\text{Fe}^{\text{II}}(\text{L})]$, M	k_{obs} , s ⁻¹		
	pH = 4.8, L = edta	pH = 4.8, L = dtpa	pH = 4.7, L = hedtra
0.005	0.0017 ± 0.0008	0.0038 ± 0.0008	0.011 ± 0.003
0.01	0.0040 ± 0.0004	0.008 ± 0.001	0.023 ± 0.002
0.015	0.0067 ± 0.0005	0.012 ± 0.002	0.032 ± 0.002
0.02	0.0093 ± 0.0004	0.015 ± 0.003	0.043 ± 0.005

^a Conditions: [total NO₂⁻] = 5 × 10⁻⁴ M; temperature 25 °C; ionic strength 0.5 M; acetic acid/acetate buffer, 0.05 M.

Table II. Values of the Pseudo-Zero-Order Rate Constant k_A as a Function of [Total NO₂⁻] and pH^a

[total NO ₂ ⁻], M	pH	k_A , M s ⁻¹
L = dtpa		
0.03	4.62	(9.97 ± 0.22) × 10 ⁻⁶
0.05	4.65	(1.7 ± 0.15) × 10 ⁻⁵
0.01	4.12	(9.5 ± 0.2) × 10 ⁻⁶
0.03	4.14	(8.7 ± 0.1) × 10 ⁻⁵
0.01	3.23	(2.6 ± 0.1) × 10 ⁻⁴
0.01	3.01	(4.5 ± 0.2) × 10 ⁻³
0.01	2.55	(1.9 ± 0.1) × 10 ⁻³
L = hedtra		
0.01	4.40	(3.03 ± 0.05) × 10 ⁻⁶
0.02	4.41	(1.22 ± 0.1) × 10 ⁻⁵
0.03	4.43	(2.25 ± 0.2) × 10 ⁻⁵
0.01	4.05	(2.9 ± 0.2) × 10 ⁻⁵
0.02	3.62	(4.6 ± 0.1) × 10 ⁻⁴
0.02	3.20	(1.96 ± 0.08) × 10 ⁻³

^a Conditions: $[\text{Fe}^{\text{II}}(\text{L})]$ = 0.001 M; temperature 25 °C; ionic strength 0.5 M; acetic acid/acetate buffer, 0.05 M for pH > 3.4.

the reaction in the absence of a buffer. The $[\text{Fe}^{\text{II}}(\text{L})]$ dependence of k_{obsd} was studied in this pH range (see Table I), and the corresponding values of k_2 are 29 ± 1 (L = edta), 51 ± 3 (L = dtpa), and 107 ± 5 M⁻¹ s⁻¹ (L = hedtra). These data once again demonstrate the significantly higher reactivity of the dtpa and hedtra complexes. In terms of the rate-determining redox reaction with HONO, it is interesting to notice that the observed sequence hedtra > dtpa > edta differs significantly from that observed for the redox reaction with O₂, viz. hedtra > edta ≫ dtpa.²¹ These redox sequences must partly be related to the driving force of the reaction expressed in terms of the redox potential of the Fe^{II}(L) species. The latter value should depend on the nature of L and the overall charge on the complex. The redox potentials (vs NHE) of Fe^{III/II}(L) are 0.12 (L = edta), 0.16 (L = dtpa), 0.33 (L = nta), and 0.77 V (L = H₂O) compared to a value of 0.99 V for the HNO₂/NO redox couple.^{24,38} On the basis of these data, the edta and dtpa complexes are expected to be significantly more reactive than the nta and aqua complexes, which is in agreement with the findings in this study. The significant difference observed especially for the reactivity of the dtpa complex in its reactions with HONO and O₂, respectively, as mentioned above, suggests that these reactions may involve significantly different redox mechanisms, i.e. outer sphere compared to inner sphere, respectively. Especially in the case of the dtpa complex, where presumably no labile water molecule is present in the coordination sphere,^{30,31} the inner-sphere mechanism will be very unfavorable and so account for the low rate constant observed for the reaction with O₂.²¹ The higher reactivity of the hedtra complex observed in both series of data must be related to the less negative charge on the ligand (compared to edta) and the presence of the -CH₂CH₂OH moiety.

When nitrite is used in excess for the complexes of edta, dtpa, and hedtra, the absorbance/time plots deviate significantly from first-order behavior (see Figure 4 in ref 10 for some typical examples in the case of L = edta). The deviations significantly depend on the pH and [total nitrite]. The absorbance/time plots

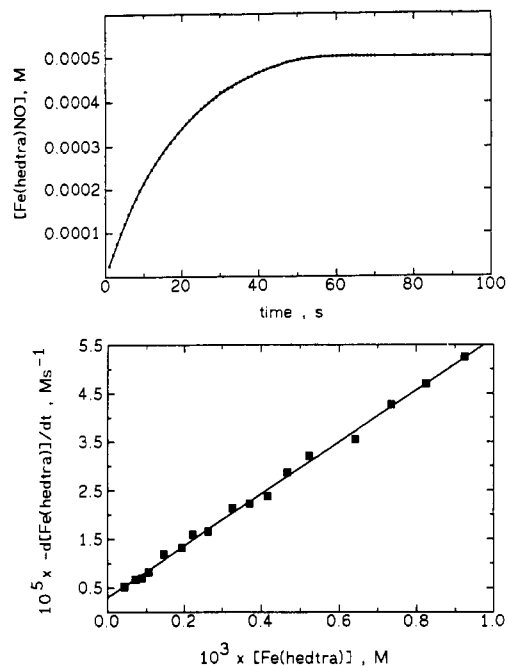


Figure 3. (a) Top: Typical plot for the formation of Fe^{II}(hedtra)NO in the presence of an excess of nitrite. Conditions: $[\text{Fe}(\text{hedtra})]$ = 0.001 M; [total nitrite] = 0.01 M; pH = 4.4. (b) Bottom: Plot of $-d[\text{Fe}(\text{hedtra})]/dt$ versus $[\text{Fe}^{\text{II}}(\text{hedtra})]$ as a function of time to calculate k_A and k_B .

Table III. Values of the Pseudo-First-Order Rate Constant k_B as a Function of [Total NO₂⁻] and pH^a

[total NO ₂ ⁻], M	pH	k_B , s ⁻¹
L = dtpa		
0.01	4.95	0.0097 ± 0.0008
0.01	4.60	0.0266 ± 0.001
0.03	4.62	0.065 ± 0.001
0.05	4.65	0.121 ± 0.003
0.03	4.14	0.238 ± 0.005
L = hedtra		
0.01	5.01	0.0202 ± 0.0004
0.02	5.03	0.033 ± 0.0007
0.03	5.05	0.046 ± 0.001
0.03	5.75	(7.9 ± 0.4) × 10 ⁻⁴
0.01	4.62	(3.6 ± 0.1) × 10 ⁻³
0.01	4.40	0.053 ± 0.001
0.02	4.41	0.108 ± 0.005
0.03	4.43	0.164 ± 0.01
0.01	4.05	0.124 ± 0.003
0.02	3.62	1.04 ± 0.04

^a Conditions: temperature 25 °C; ionic strength 0.5 M; acetic acid/acetate buffer, 0.05 M.

in general consist of an initial first-order and subsequent zero-order contribution. The contribution of the zero-order reaction increases with decreasing pH, and the zero-order curve exhibits a sudden inflection (dead end) when the final absorbance is reached. According to the method developed previously,¹⁰ such absorbance/time plots were converted to concentration/time plots, and the reaction rate, expressed as $-d[\text{Fe}^{\text{II}}(\text{L})]/dt$ (calculated from the $[\text{Fe}^{\text{II}}(\text{L})\text{NO}]$ produced during the reaction), was estimated as a function of $[\text{Fe}^{\text{II}}(\text{L})]$. A plot of $-d[\text{Fe}^{\text{II}}(\text{L})]/dt$ versus $[\text{Fe}^{\text{II}}(\text{L})]$ during the course of the reaction (for a typical example see Figure 3) permits the calculation of the first-order constant from the slope and the zero-order rate constant from the intercept. Such plots exhibit an increasing intercept and decreasing slope when the zero-order contribution increases at lower pH and higher [total NO₂⁻].¹⁰ The resulting rate constants (k_A and k_B) are summarized in Tables II and III for L = dtpa and hedtra, respectively.

The observed first-order rate constants k_B exhibit a linear dependence on [HONO] when the data in Table III and those

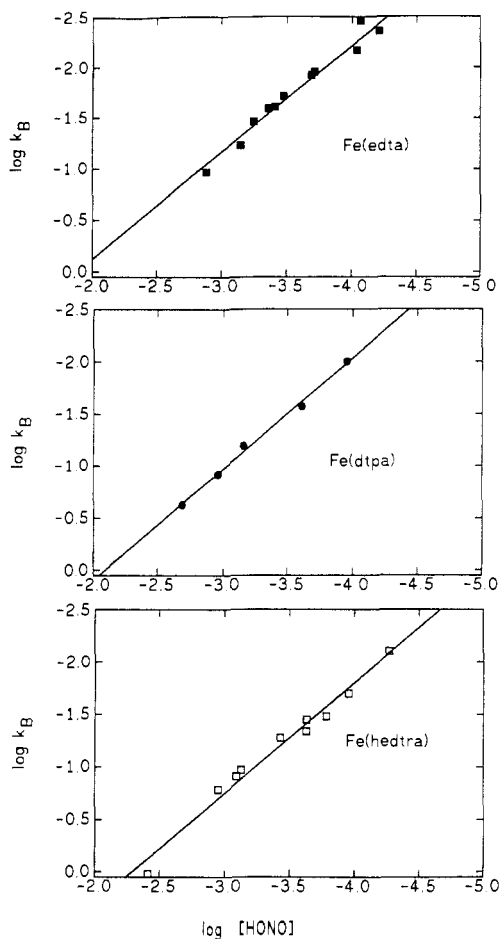
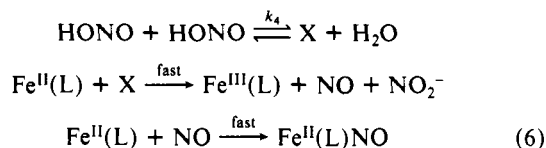


Figure 4. Plots of $\log k_B$ versus $\log [\text{HONO}]$ for the data in Table II and the literature.¹⁰

reported previously¹⁰ are plotted as $\log k_B$ versus $\log [\text{HONO}]$ as shown in Figure 4. The plots all exhibit a unity slope, viz. 1.04 ± 0.04 ($L = \text{edta}$), 1.06 ± 0.05 ($L = \text{dtpa}$), and 1.05 ± 0.06 ($L = \text{hedtra}$). Under these conditions the mechanism in (2) results in the rate equation (5), and the intercepts in Figure 4 can be used

$$-d[\text{Fe}^{\text{II}}(\text{L})]/dt = k_B[\text{Fe}^{\text{II}}(\text{L})] = 2k_2[\text{Fe}^{\text{II}}(\text{L})][\text{HONO}] \quad (5)$$

to estimate k_2 . The values of k_2 , viz. 45 ± 8 ($L = \text{edta}$), 85 ± 11 ($L = \text{dtpa}$), and $125 \pm 20 \text{ M}^{-1} \text{ s}^{-1}$ ($L = \text{hedtra}$), are in close agreement with those reported above for $\text{Fe}^{\text{II}}(\text{L})$ in excess and once again demonstrate the same reactivity pattern. The observed zero-order rate constants k_A also exhibit a characteristic dependence on the $[\text{HONO}]$, as demonstrated by the plots of $\log k_A$ versus $\log [\text{HONO}]$ in Figure 5. The slopes of these plots, 1.97 ± 0.02 ($L = \text{edta}$), 2.16 ± 0.11 ($L = \text{dtpa}$), and 2.09 ± 0.14 ($L = \text{hedtra}$), demonstrate that k_A exhibits a second-order dependence on the $[\text{HONO}]$. To account for this dependence, we suggest the rate-determining formation of an intermediate species X under these conditions as shown in (6), where X can be visualized as



N_2O_3 .¹⁰ This intermediate is a more effective redox partner for $\text{Fe}^{\text{II}}(\text{L})$ than HONO and will only be produced at low pH and in the presence of an excess of nitrite, that is where $[\text{HONO}]$ is high. Under these conditions the rate law is given by (7), from

$$-d[\text{Fe}^{\text{II}}(\text{L})]/dt = k_A = 2k_4[\text{HONO}]^2 \quad (7)$$

which it follows that the limiting rate constant k_4 can be calculated from the intercept of the plots in Figure 5. The corresponding values for k_4 are 31 ± 6 ($L = \text{edta}$), 28 ± 5 ($L = \text{dtpa}$), and 25

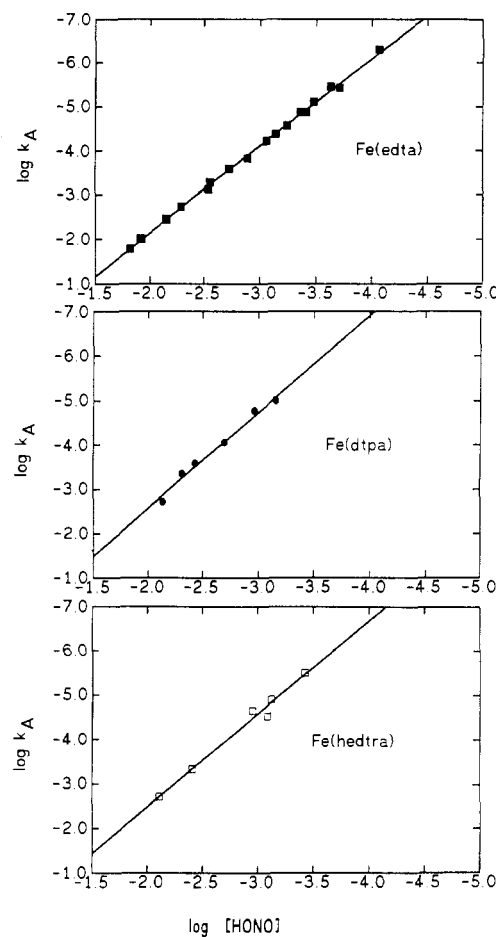
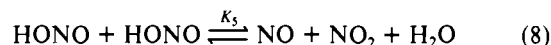
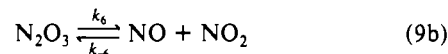
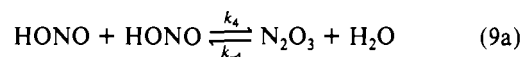


Figure 5. Plots of $\log k_A$ versus $\log [\text{HONO}]$ for the data in Table III and the literature.¹⁰

$\pm 6 \text{ M}^{-1} \text{ s}^{-1}$ ($L = \text{hedtra}$) and are independent of L , as would be expected for such a rate-determining step. In addition, these values are in excellent agreement with those reported in the literature, viz. 43, 14, and $13.4 \text{ M}^{-1} \text{ s}^{-1}$,³⁹⁻⁴¹ although the reaction is formulated slightly differently in the literature as shown in (8).



Grätzel and co-workers⁴¹ included N_2O_3 as an intermediate as shown in (9) and found with aid of pulse radiolysis techniques



values for $K_6 = k_6/k_{-6} = 7.3 \times 10^{-5} \text{ M}$ and $k_{-4} = 530 \text{ s}^{-1}$. The latter value combined with $K_5 = k_4K_6/k_{-4} = 6.1 \times 10^{-6}$ ⁴² results in $k_4 = 44.3 \text{ M}^{-1} \text{ s}^{-1}$, which is again within the range of values reported above. It follows that our experimental values for k_4 are in good agreement with these values, especially when the indirect way of determination is taken into account. However, it is important to note that we suggest the formation of a reactive intermediate, most probably N_2O_3 , that reacts with $\text{Fe}^{\text{II}}(\text{L})$, to produce $\text{Fe}^{\text{III}}(\text{L})$ and NO , followed by the rapid formation of $\text{Fe}^{\text{II}}(\text{L})\text{NO}$. This suggestion is based on our observation that $\text{Fe}^{\text{III}}(\text{L})$ and $\text{Fe}^{\text{II}}(\text{L})\text{NO}$ are produced in the ratio 1:1 also under these conditions.

The overall mechanism, which consists of reactions 2 and 6, can account for the mixed-order dependence observed in the

(39) Ram, M. S.; Stanbury, D. M. *J. Am. Chem. Soc.* **1984**, *106*, 8136.

(40) Garley, M. S.; Stedman, G. *J. Inorg. Nucl. Chem.* **1981**, *43*, 2863.

(41) Grätzel, M.; Taniguchi, S.; Henglein, A. *Ber. Bunsen-Ges. Phys. Chem.* **1970**, *74*, 488.

(42) Lee, Y. N.; Schwartz, S. E. *J. Geophys. Res.* **1981**, *86*, 971.

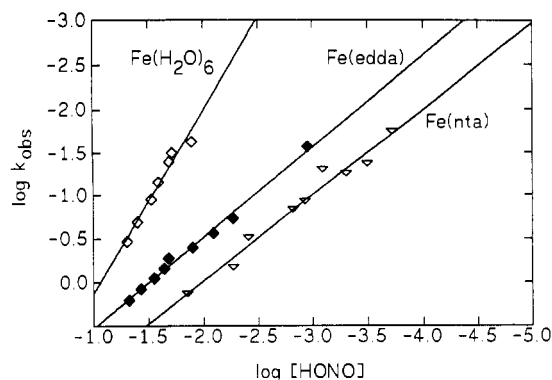


Figure 6. Plots of $\log k_{\text{obs}}$ versus $\log [\text{HONO}]$ for the data in Table IV.

presence of excess nitrite as indicated by the overall rate equation given in (10). At high pH and low nitrite concentration, k_2 is

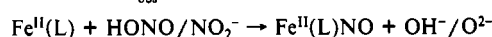
$$-d[\text{Fe}^{\text{II}}(\text{L})]/dt = k_A + k_B[\text{Fe}^{\text{II}}(\text{L})] = 2k_4[\text{HONO}]^2 + 2k_2[\text{Fe}^{\text{II}}(\text{L})][\text{HONO}] \quad (10)$$

rate-determining and a pseudo-first-order behavior is observed. However, as the reaction proceeds, $[\text{Fe}^{\text{II}}(\text{L})]$ decreases and the rate of the process in (2) decreases to the point that the pseudo-zero-order path in (6) contributes substantially. It follows that the latter path will play a prominent role at lower pH and higher nitrite concentration, i.e. where $[\text{HONO}]$ is significant. This situation will not show up in the presence of excess $\text{Fe}^{\text{II}}(\text{L})$, accounting for the fact that no such deviations were observed under these conditions.

The corresponding nta and edda systems exhibit a different behavior. In the presence of excess nitrite, the absorbance/time plots do not show any deviation from pseudo-first-order behavior. The plots of $\log k_{\text{obs}}$ versus $\log [\text{HONO}]$ are linear (see Figure 6), with slopes 0.99 ± 0.02 ($L = \text{nta}$) and 1.04 ± 0.04 ($L = \text{edda}$), and demonstrate the first-order dependence on $[\text{HONO}]$. The values of k_2 calculated from the intercepts of these plots according to eq 5 are 44 ± 8 ($L = \text{nta}$) and $19 \pm 2 \text{ M}^{-1} \text{ s}^{-1}$ ($L = \text{edda}$) and demonstrate the lower reactivity of these complexes compared to the dtpa and hedtra species. Presumably chelation and charge effects control the redox potential of these complexes and also the value of k_2 , as mentioned before. It follows that the reactions given in (2) adequately describe the behavior of these complexes. On the other hand, there must be a good reason for the fact that the pseudo-zero-order reaction path does not contribute to the overall process for these two ligands. We suggest that the subsequent reaction of $\text{Fe}^{\text{II}}(\text{L})$ with X in (6) may be significantly slower for these complexes and prevent the effective participation of this reaction path. Kinetic simulations⁴³ demonstrated that the pseudo-zero-order contribution will only become observable when the rate constant of this subsequent step (i.e. second reaction in (6)) is larger than $10^4 \text{ M}^{-1} \text{ s}^{-1}$. This means that the overall contribution of the pseudo-zero-order reaction paths seems to be controlled by the magnitude of the rate constant of the subsequent reaction in (6). A further reason for this deviation may lie in the fact that more vacant coordination sites are available for $L = \text{nta}$ and edda. In this respect, it is interesting to note that the partial formation of $\text{Fe}(\text{nta})(\text{NO})_2$ has been suggested in the case of the nta complex,²³ which could also affect the nature of the overall mechanism. We could not find any direct evidence for the formation of such a species in our investigations and have therefore not included this possibility in the suggested reaction mechanism.

We now turn to a discussion of the results obtained for the system with $L = \text{H}_2\text{O}$, i.e. $\text{Fe}(\text{H}_2\text{O})_6^{2+}/\text{NO}/\text{HONO}/\text{NO}_2^-$. Of the series of complexes studied, this system is the most complicated, although probably the most relevant, one in terms of atmospheric oxidation processes. Fundamental aspects concerning this system have been presented in detail elsewhere.^{17,44-47} Bonner et al.^{46,47}

Table IV. Values of k_{obs} for the Reaction^a



pH	[total NO_2^-], M	k_{obs} , s^{-1}
$L = \text{nta}$		
4.78	0.03	0.056 ± 0.001
4.75	0.02	0.043 ± 0.001
4.70	0.01	0.018 ± 0.002
4.62	0.05	0.12 ± 0.001
4.09	0.02	0.15 ± 0.001
4.06	0.01	0.05 ± 0.003
3.45	0.02	0.68 ± 0.008
3.19	0.01	0.31 ± 0.01
2.60	0.02	1.36 ± 0.03
$L = \text{edda}$		
4.67	0.05	0.027 ± 0.003
3.92	0.05	0.187 ± 0.006
3.71	0.05	0.274 ± 0.012
3.47	0.05	0.401 ± 0.027
3.15	0.05	0.53 ± 0.02
3.07	0.05	0.71 ± 0.03
2.88	0.05	0.92 ± 0.08
2.54	0.05	1.20 ± 0.05
1.72	0.05	1.6 ± 0.1
$L = \text{H}_2\text{O}$		
3.14	0.03	0.0233 ± 0.002
2.81	0.03	0.0318 ± 0.002
2.67	0.03	0.0403 ± 0.004
2.22	0.03	0.0705 ± 0.003
1.00	0.05	0.341 ± 0.025
0.94	0.04	0.204 ± 0.014
0.90	0.03	0.113 ± 0.003

^a $[\text{Fe}^{\text{II}}(\text{L})] = 0.001 \text{ M}$ for $L = \text{nta}, \text{edda}$; $[\text{Fe}^{\text{II}}(\text{H}_2\text{O})_6] = 0.002 \text{ M}$; acetic acid/acetate buffer, 0.05 M for $\text{pH} > 3.4$; ionic strength 0.5; temperature 25 °C.

performed a detailed kinetic study of the reduction of nitric oxide by Fe(II) and reported evidence for the participation of a pH-dependent dinitrosyl complex bearing both formal NO^+ and formal NO^- in a cis relation. It was therefore not our intention to perform a detailed study of this system but, merely by way of comparison, some experiments similar to those for the chelated metal center. The reaction of $\text{Fe}(\text{H}_2\text{O})_6^{2+}$ with $\text{NO}(\text{aq})$ is significantly less effective than for the other investigated complexes, as reflected by the K_1 value of 470 M^{-1} mentioned previously,^{6,48} but still occurs in the milli- and microsecond time range. During the reaction with $\text{HONO}/\text{NO}_2^-$, Fe(III) species are produced that precipitate at $\text{pH} > 3.3$ due to the formation of hydroxo species.⁷ It was therefore essential to work in an acidic medium ($\text{pH} < 3.2$), which naturally made the system significantly different compared to the other investigated complexes. In the presence of an excess $\text{HONO}/\text{NO}_2^-$, the main reaction observed exhibits good first-order behavior and the corresponding rate constant shows a linear dependence on $[\text{HONO}]^2$. This is demonstrated by the plot of $\log k_{\text{obs}}$ versus $\log [\text{HONO}]$ in Figure 6, for which the slope is 2.11 ± 0.18 and the intercept $174 \pm 23 \text{ M}^{-2} \text{ s}^{-1}$. The square dependence on $[\text{HONO}]$ may indicate that either the first equilibrium in (6), i.e. the production of X, or the overall equilibrium (8) plays an important role during this reaction. In addition, the observed pseudo-first-order kinetics requires that the subsequent step involving Fe(II) must be rate-determining,^{17,39,45} which means that the formation of N_2O_3 cannot be the rate-determining step as found for the edta, dtpa, and hedtra complexes. The reaction of Fe(II) with N_2O_3 should, on the basis of our other data, be significantly more effective than the reaction with HONO or NO under the present conditions. The high redox potential of the Fe(III)/II system presumably accounts for the absence of the direct reaction with HONO as outlined in (2). Under these

(43) Braun, W.; Herron, J. T.; Kahaner, D. K. *Int. J. Chem. Kinet.* **1988**, *20*, 51.

(44) Abel, E.; Schmid, H.; Pollak, F. *Monatsch. Chem.* **1936**, *69*, 125.

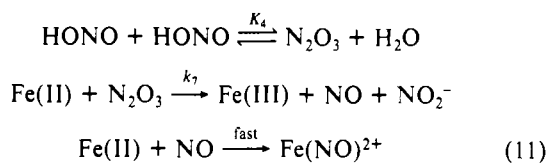
(45) Orban, M.; Epstein, I. R. *J. Am. Chem. Soc.* **1982**, *104*, 3918.

(46) Bonner, F. T.; Pearsall, K. A. *Inorg. Chem.* **1982**, *21*, 1973.

(47) Pearsall, K. A.; Bonner, F. T. *Inorg. Chem.* **1982**, *21*, 1978.

(48) Kustin, K.; Taub, I. A.; Weinstock, E. *Inorg. Chem.* **1966**, *5*, 1079.

conditions the overall scheme can be summarized by the reactions in (11), for which the corresponding rate law is given in (12). This



$$-d[\text{Fe(II)}]/dt = 2k_7K_4[\text{HONO}]^2[\text{Fe(II)}] \quad (12)$$

suggestion is also in agreement with our findings for the nta and edda complexes, since the first-order reaction path outlined in (2) is more effective due to the significantly lower redox potentials of these complexes. The reaction product is quoted as Fe(NO)_2^{2+} in (11), but does not rule out the formation of Fe(NO)_2^{2+} as suggested in the literature.^{46,47} This could, for instance, occur in a subsequent fast reaction involving Fe(NO)_2^{2+} and HONO or NO. However, no evidence for the formation of Fe(NO)_2^{2+} under our selected experimental conditions could be found. It follows that the intercept of the plot in Figure 6 represents $2k_7K_4$, such that $k_7 = 1 \times 10^3 \text{ M}^{-1} \text{ s}^{-1}$, since $K_4 = 8.4 \times 10^{-2} \text{ M}^{-1}$.^{41,42} The value of k_7 is very reasonable, considering the limit of $10^4 \text{ M}^{-1} \text{ s}^{-1}$ predicted for the nta and edda complexes in the previous section. An overall comparison of the results reported for the series of complexes investigated in this study reveals a few interesting tendencies. Obviously, the redox potential of the $\text{Fe}^{\text{II/III}}(\text{L})$ system is not the only important factor. In addition, the overall charge on the complex, the availability of vacant coordination sites and

the possible changeover between outer-sphere and inner-sphere redox mechanisms must be taken into consideration. The overall observed effect is a composite of various contributing factors, which may vary from system to system. Nevertheless, the observed trends seem to fall in with the basic concepts of coordination chemistry in terms of the labilization by chelation on the one hand and steric blocking on the other. The direct reaction between $\text{Fe}^{\text{II}}(\text{L})$ and NO seems to be very similar for all L and is mainly controlled by the lability of the complex and the availability of coordinate solvent molecules presumably undergoing a rapid substitution reaction with NO. The parallel reaction path involving HONO/NO_2^- is more complicated and exhibits larger variations with L, since it involves an electron-transfer process with HONO or N_2O_3 during which $\text{Fe}^{\text{III}}(\text{L})$ and NO are produced. The observed kinetics and their dependence on pH and [HONO] differ significantly for various L. Again, the availability of labile coordination sites and the redox chemistry involved will determine the overall magnitude of this contributing reaction path.

The systematic variation of L has enabled us to investigate the possible influence of this aspect on the overall process involving the simultaneous removal of SO_2 and NO_x from flue gases of coal-fired power plants, as mentioned in the Introduction. The subsequent reactions of the produced $\text{Fe}^{\text{II}}(\text{L})\text{NO}$ species with $\text{HSO}_3^-/\text{SO}_3^{2-}$ and the overall catalytic role of the $\text{Fe}^{\text{II}}(\text{L})$ species will be reported in a forthcoming paper.

Acknowledgment. We gratefully acknowledge financial support from the Deutsche Forschungsgemeinschaft, Fonds der Chemischen Industrie, and Max-Buchner Forschungsförderung.

Contribution from the Bristol-Myers Squibb Pharmaceutical Research Institute, New Brunswick, New Jersey 08903-0191

pH Dependence of Relaxivities and Hydration Numbers of Gadolinium(III) Complexes of Linear Amino Carboxylates

C. Allen Chang,* Harry G. Brittain, Joshua Telser, and Michael F. Tweedle

Received January 11, 1990

Spin-lattice relaxivity values (R_1 , 20 MHz, 40 °C) for Gd(III) complexes and the number of inner-sphere-coordinated water molecules (q , hydration number) in analogous Tb(III) complexes were determined for a series of Gd(III) and Tb(III) amino carboxylate complexes. The observed relaxivity values were found to decrease with increasing pH in the acid region below pH 7. When a Gd(III) complex became fully formed, the relaxivity value became invariant, and this limiting value correlated well with the number of inner-sphere-coordinated water molecules for mononuclear species. Gd(III) complexes of ligands with more donor atoms tended to have lower q and R_1 . The observed order of R_1 (and q) values were found to be as follows: $\text{Gd}^{3+}(\text{aq})$ (9) > $\text{Gd}(\text{HEDTA})$ (4) > $\text{Gd}(\text{EDTA})^-$ (3) > $\text{Gd}(\text{DTPA})^{2-}$ (1) = $\text{Gd}(\text{EGTA})^-$ (1) > $\text{Gd}(\text{TTHA})^{2-}$ (0). The outer-sphere relaxivity for these complexes is estimated to be $2.2 \pm 0.1 \text{ (mM s)}^{-1}$ and each inner-sphere-coordinated water adds approximately $1.6 \pm 0.1 \text{ (mM s)}^{-1}$. Deviations from linearity were observed for TTHA complexes at pH 4-5 and for HEDTA at and above pH 10. The increased relaxivity per complex in these cases is rationalized in terms of an oligomerization, independently observed spectroscopically, which then results in either increased τ_r and/or an increase in the magnetic moment that each water proton experiences.

Introduction

Gadolinium(III) complexes of polyamino polycarboxylate ligands are currently used clinically as magnetic resonance imaging (MRI) contrast agents. A practical MRI contrast agent must remain intact under physiological conditions so as to minimize the concentrations of free metal and ligand, which are poorly tolerated, while strongly affecting the spin-lattice relaxation time (T_1) of bulk solvent water.¹ The former is best accomplished through the use of a strongly binding ligand that occupies most of the available coordination sites of the metal, while the latter occurs most effectively with a maximal hydration state of the Gd(III) ion. These conflicting requirements necessitate careful ligand design, as well as study of Gd(III) complex stability, dissociation kinetics, and relaxivity under a variety of conditions.

The stability (as measured by complex formation constants), dissociation kinetics, spin-lattice relaxivity (R_1 , the second-order rate constant that describes catalysis of T_1 relaxation, vide infra), and inner-sphere hydration number (q , the number of coordinated water molecules) are particularly dependent on the solution pH. At low pH values, the coordinating carboxylate groups become protonated, leading to at least partial dissociation of the complex. Within this pH range, the resulting hydration number will be relatively high. At sufficiently high pH values, coordination of hydroxide ion can occur. This reduces rapid exchange with solvent water and may allow oligomers to form. Both factors may decrease or increase relaxivity.

Relaxivities and inner-sphere hydration states of Gd(III) and Tb(III) complexes of linear amino carboxylic acids were determined as a function of pH to better understand these effects. The ligand systems studied were EDTA (ethylenediaminetetraacetic acid), HEDTA (*N*-(2-hydroxyethyl)ethylenediaminetriacetic acid),

(1) Lauffer, R. B. *Chem. Rev.* 1987, 87, 901.